UCLA
UCLA Electronic Theses and Dissertations

Title

High Voltage DC/DC Converters for Electrostatic Energy Storage System

Permalink

https://escholarship.org/uc/item/5dz2720r

Author

Xiang, Tianyu

Publication Date

2024

Peer reviewed|Thesis/dissertation

UNIVERSITY OF CALIFORNIA

Los Angeles

High Voltage DC/DC Converters for Electrostatic Energy Storage System

A thesis submitted in partial satisfaction

of the requirements for the degree Master of Science

in Electrical & Computer Engineering

by

Tianyu Xiang

2024

ABSTRACT OF THE THESIS

High Voltage DC/DC Converters for Electrostatic Energy Storage System

by

Tianyu Xiang

Master of Science in Electrical & Computer Engineering

University of California, Los Angeles, 2024

Professor Subramanian Srikantes Iyer, Chair

The increasing demand for clean and sustainable energy sources necessitates effective

energy storage solutions. This thesis proposes a decentralized approach to energy storage by

utilizing high-density rolled polymer-based capacitors. The objective is to address the

intermittent nature of renewable energy generation and develop a storage system that is

affordable, sustainable, and easily deployable. Conventional capacitors typically do not

exhibit high energy capacity. Therefore, this research emphasizes optimizing surface area,

implementing high voltage storage capabilities (up to 3 kV), and utilizing a polymeric

material with a high dielectric constant. By focusing on these factors, the research aims to

overcome the limitations of conventional capacitors and develop a storage system with significantly increased energy density, enabling more efficient energy storage for clean and sustainable sources. This thesis presents the design and implementation of a high-efficiency DC/DC converter system for energy storage applications. The system utilizes a transformer less step-up converter and a flyback topology for step-down conversion. The transformer less step-up converter is designed to increase the input voltage efficiently, while the flyback topology is employed for effective voltage reduction. Both converters achieve an impressive efficiency of 90%. The proposed solution addresses the challenges of energy conversion in storage systems, ensuring both reliability and performance.

The thesis of Tianyu Xiang is approved.

Rajit Gadh

Gaurav Sant

Subramanian Srikantes Iyer, Committee Chair

University of California, Los Angeles

2024

TABLE OF CONTENTS

LIST OF FIGURES

LIST OF TABLES

ACKNOWLEDGEMENTS

First, I am grateful to Prof. Subramanian S. Iyer for his invaluable guidance and unwavering support throughout this research project. He initiated the project ideas, assembled our team, and provided enthusiastic academic assistance.

I also extend my gratitude to Prof. Rajit Gadh and Prof. Gaurav Sant for their valuable time and service as members of my thesis committee.

Special thanks to Haoxiang Ren, Randall Irwin, Tak Fukushima, and my colleagues at CHIPS lab, as well as Niharika Tripathi and Harshit Ranjan, for their invaluable assistance and support throughout the research project.

I sincerely appreciate the encouragement and constructive environment provided by all my lab members.

Lastly, I am deeply thankful to my family and friends for their unconditional love and unwavering support, without which this journey would not have been possible.

CHAPTER 1: INTRODUCTION

1.1 Motivation

The utilization of renewable energy sources like solar, wind, and tidal power has garnered significant attention due to their sustainable nature. However, a major drawback of these sources lies in their inherent intermittency. Current approaches to address this intermittency primarily rely on electrochemical (batteries) and mechanical (water storage tanks, flywheels, etc.) energy storage methods. Despite their widespread use, these methods are not without their limitations. They often exhibit environmental concerns and tend to be centralized, relying on a well-connected electrical grid. Moreover, the process of transduction from electrical energy to other forms introduces inefficiencies.

The imperative for innovative energy storage solutions has become increasingly apparent, driven by the challenges associated with the intermittent nature of renewable energy sources. In response to this need, this thesis introduces a novel decentralized strategy for storing electrical energy derived from renewables. Our approach revolves around the electrostatic storage of substantial energy quantities at elevated voltages on rolled polymer-based capacitors. This innovative method aims to enhance both the accessibility and efficiency of renewable energy utilization with minimal costs.

Figure 1-1 depicts an innovative approach to an electrostatic energy storage system. This system utilizes flexible rolled-up capacitors to store energy at high densities, specifically at voltages ranging from 5 kV to 10 kV. The design is environmentally friendly and aims for underground distribution to locally supply electrical energy, making it cost-effective for households.

The system operates by initially receiving intermittent power input at low voltages, which is then converted to higher voltages using a high-efficiency power converter. This elevated voltage is utilized to charge flexible capacitor cells, tightly wound according to the dimensions detailed in Table 1-1. Subsequently, the stored high voltage on the capacitors can be converted to lower voltages as required by specific applications.

Dimension of the cell	Units (mm)
Height	1000
Outer Diameter	1000
Inner Diameter	200
Number of turns	1000
Turn spacing	0.2

Table 1-1 Dimensions of the rolled-up capacitor.

The energy E stored in a capacitor is given by $E = \frac{1}{2}*C*V^2$, where C is the capacitance and V is the voltage across the capacitor. The capacitance C is determined by $C = k* \varepsilon 0*A/d$, where k is the dielectric constant of the material, epsilon 0 is the permittivity of vacuum, A is the area of the capacitor's electrodes, and d is the distance between the electrodes (thickness of the dielectric).

Thus, the electrostatic energy stored can be increased by selecting a material with a higher dielectric constant k increasing the applied voltage V, enlarging the electrode area A, reducing the dielectric thickness d, or employing a combination of these factors. The relationship shows that the stored electrostatic energy E linearly depends on k, A, and V under a constant electric

field. The relationship can be expressed as $E = 1/2 * \varepsilon 0 * A(V/d) * V$, where the electric field is influenced by both the applied voltage and the dielectric thickness.

The flexible, rolled capacitors essential for this electrostatic energy storage system must utilize dielectrics capable of enduring high voltages over extended periods.
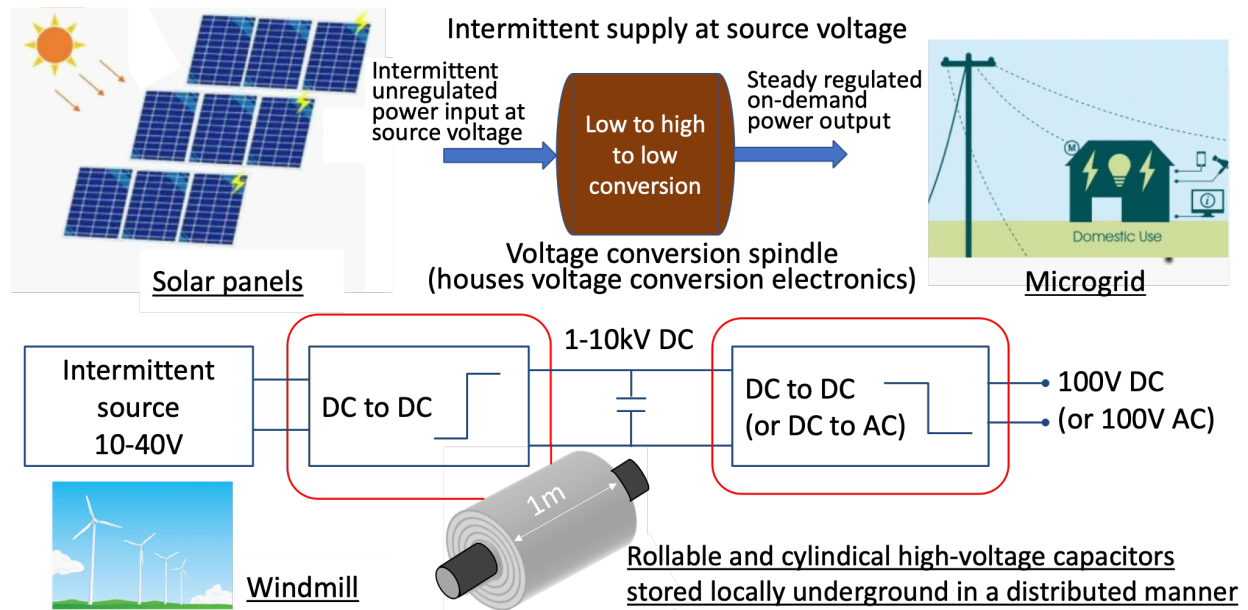
Figure 1-1 Schematic of a new energy storage system with rollable high-voltage large-volume capacitors stored locally underground in a distributed manner.

Our approach involves employing a multivariate optimization strategy, which includes modifying the surface area, utilizing high voltage storage via transformers and converters, and incorporating a high dielectric constant polymer material to achieve high energy density. This paper focuses on the design and testing of a low-to-high-to-low voltage converter.

CHAPTER 2: BACKGROUND AND LITERATURE REVIEW

2.1 Introduction

In recent years, there has been extensive research on high voltage gain DC/DC converters, spurred by advancements in semiconductor technology since the 1950s. These converters play a critical role in HVDC transmission and applications requiring low input voltages. While conventional boost converters effectively raise voltage levels, they face challenges such as extreme duty ratios and high stress on switches when the duty cycle approaches unity or zero, complicating the maintenance of a stable output voltage amidst load variations and external disturbances[2].

This section explores several methods to improve voltage step-up conversion ratios. Transformer-based DC/DC converters achieve significant ratios by adjusting the turns ratio between secondary and primary windings[2]. However, large turns ratios introduce leakage inductance, leading to voltage spikes and necessitating high-rated switches with substantial on-state resistance, resulting in increased conduction losses. Alternatively, using passive components like capacitors and inductors can boost voltage by storing and releasing energy in series with the input voltage, thereby achieving higher output voltages[3].

Furthermore, employing multiple converters can further enhance voltage gains. For example, cascading boost converters or employing parallel-input series-output configurations can increase the overall voltage step-up ratio.

This chapter categorizes converters based on their topologies, operating principles, and applications. It also reviews various DC/DC converters known for their high voltage conversion

ratios, discussing control methods, switching strategies, and failure mechanisms associated with semiconductor components.

2.2 Isolated/Non-isolated Converters

DC/DC converters are classified into isolated and non-isolated types based on whether they provide galvanic isolation using transformers, as depicted in Figure 2.2. These converters can operate with either voltage-fed or current-fed input power. On the output side, they can drive loads such as devices or grid-tied inverters. Switching converter modules employ active switches like MOSFETs, alongside passive components such as inductors, capacitors, and diodes [4].

Isolated DC/DC converters utilize high-efficiency transformers to achieve galvanic isolation and impedance matching between the input source and output load. This isolation is critical for preventing safety hazards. The conversion process involves initially converting DC input power to AC using a switching module, which is then transferred across the transformer via electromagnetic fields to achieve isolation. A rectifier is used to convert AC back to DC for powering the load. Adjusting the transformer's turns ratio further increases the output voltage, but this can lead to leakage inductance and voltage spikes on electronic components. However, the inclusion of transformers increases the converter's size, weight, and power loss [4].

Non-isolated converters, on the other hand, offer advantages such as lower cost, high efficiency, and high-power density due to their simpler design and lack of transformers. These converters typically use switched capacitors or inductors to achieve high output voltages. Furthermore, the size and weight of passive components like inductors and capacitors decrease as the operating frequency increases [4]. Thus, increasing the operating frequency, typically ranging from tens of kilohertz to hundreds of kHz, can further reduce the size of non-isolated converters. However, in high-power

applications, non-isolated converters may experience significant heat loss and lower reliability due to magnetic saturation of inductors.
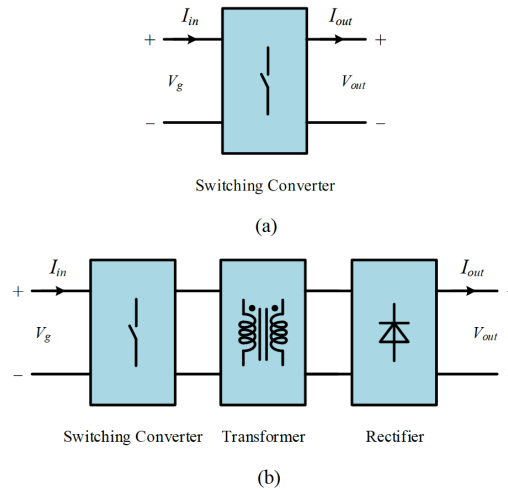
Figure 2-1 Schematic of non-isolated and isolated converters: (a) non-isolated; (b) isolated.

2.3 Categories of Voltage Boost DC/DC Converters and Regulators

2.3.1　Linear Regulator

The linear regulator, depicted in Figure 2.1, operates using a high-gain amplifier with negative feedback. Unlike a switch, its output transistor remains active, regulated by a stable voltage reference (VR) fed into the amplifier's non-inverting input. This configuration forms a shunt-series feedback loop, resulting in Vo = (1 + R1/R2) * VR.

However, its primary drawback is low efficiency, especially with larger dropout voltages (Vin − Vo). Limited to step-down conversion, if input voltage falls below a threshold, regulation fails, causing output voltage to drop below nominal levels. Some commercial versions, termed low-dropout regulators (LDOs), use PMOS pass transistors to minimize dropout voltage. Yet, efficiency is capped by Vin − Vout > Veff, restricting maximum efficiency.

Modern LDOs also provide good line/load regulation and high power-supply-rejection (PSR) for noise attenuation (Patel and Rincon-Mora, 2010), using current-mode designs to heighten PSR via a sampling feedback loop. Although straightforward to implement, linear regulators' efficiency scales roughly with (Vo/Vin), challenging design as lower supply voltages emerge. Consequently, switching regulators often replace linear types for enhanced efficiency.

2.3.2 Charge Pump or Switched Capacitor Converter

The switched capacitor (SC) converter, illustrated in Figure 2.2, operates by charging and discharging capacitor C1 in complementary phases, CLK+ and CLK−, to maintain an output voltage Vo close to 2Vin, hence it is also referred to as a voltage doubler. During CLK+ phase, C1's upper plate connects to Vin while the lower plate connects to ground. In CLK− phase, C1 connects between Vin and intermediate output Vo1, boosting output voltage to 2Vin. For better regulation and reduced switching noise, a low-dropout regulator (LDO) typically follows the charge pump to generate final output voltage Vo. Non-overlapping CLK+ and CLK− signals prevent short-circuit currents, minimizing power loss.
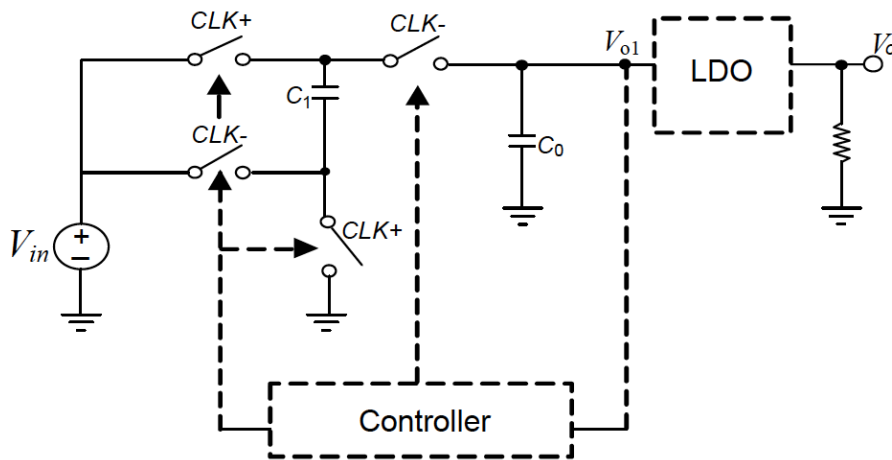
Figure 2-2 The switched capacitor converter

This topology can also function as a step-down converter by reversing power flow direction. SC converters are capable of moderate output currents and can generate negative voltages by inverting output capacitor nodes. Regulation can be achieved through an LDO or charge pump modulation circuitry. LDO regulation ties efficiency closely to input-output voltage ratio, potentially limiting efficiency. Conversely, charge pump modulation introduces output resistance $R = a^2/(2*f*C)$, where C is capacitor value, a is charge multiplier, and f is switching frequency, impacting SC converter efficiency. Large capacitor arrays mitigate output impedance for higher efficiency.

2.3.3   Switched-mode DC-DC Converter

Switched-mode DC-DC converters, the third type of regulator, come in various topologies such as buck, boost, and buck-boost, which are the most fundamental designs. These converters offer the highest efficiency among regulator types and can handle high output currents. While theoretically capable of 100% efficiency, practical limitations due to component losses typically cap efficiency around 90%.

DC-DC converters are known for their output ripple and switching noise, which are drawbacks compared to other regulators. They also tend to be more expensive because they require external components like inductors and capacitors. However, advancements in technology have led to higher switching frequencies, reducing the size and cost of these components.

Buck (Step-Down) Converter (a)   Boost (Step-Up) Converter (b)   Buck-Boost Converter (c)
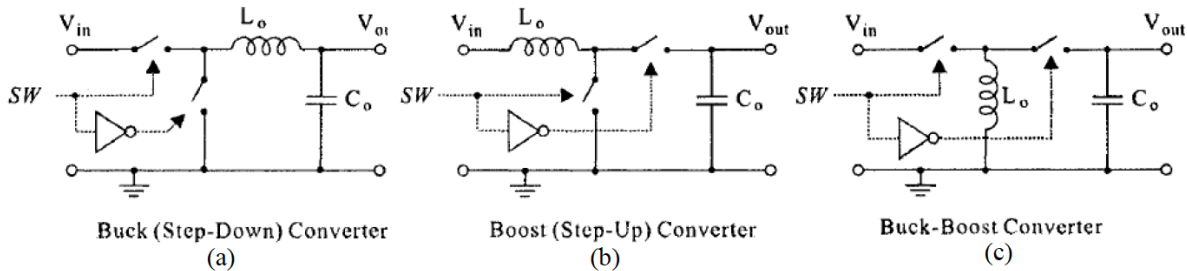
Figure 2-3 illustrates basic configurations of buck, boost, and buck-boost converters, where SW denotes the switching signal (controller not shown).

	Linear Regulator	Switched Capacitor Converter	DC-DC Converter
Advantages	Simple Reliable Inexpensive	Moderate efficiency and cost	Variety (step-down or step-up) High efficiency (80% $\sim$ 98%)
Disadvantages	Only step-down Low efficiency	Slow response	Complex Costly
Applications	Low current and input voltage Suitable for sensitive circuit	Medium current operation	High current and input voltage

Table 2-1 Advantages and Disadvantages of 3 Categories of Voltage Regulators

In order to reduce energy loss, we pursue a DC/DC Converter in the design because of its higher efficiency.

CHAPTER 3: METHODOLOGY

3.1 Purpose and Goal

The aim of this project is to explore various methods for designing DC/DC converters that are suitable for high voltage low current applications for the energy storage project. The investigation will be conducted using established topologies and will primarily consist of LTspice simulations. The converters will be evaluated mainly based on output voltage, efficiency, power, size, cost and reliability.

Step up DC-DC Converter:

1. Input voltage: 12–48V

2. Output voltage: 1000–3000V

3. Output power: ≈1.5W

4. Efficiency: >85%

5. Less price and size

Step down DC-DC Converter:

1. Input voltage: 3000V

2. Output voltage: 24V-110V

3. Output power: ≈1.5W

4. Efficiency: >85%

5. Less price and size

3.2 Conventional Primary Design: Step up DC/DC Converter

The circuit in figure 3-1 is convert 24V to 2.5 kV while powering a 420mW load.
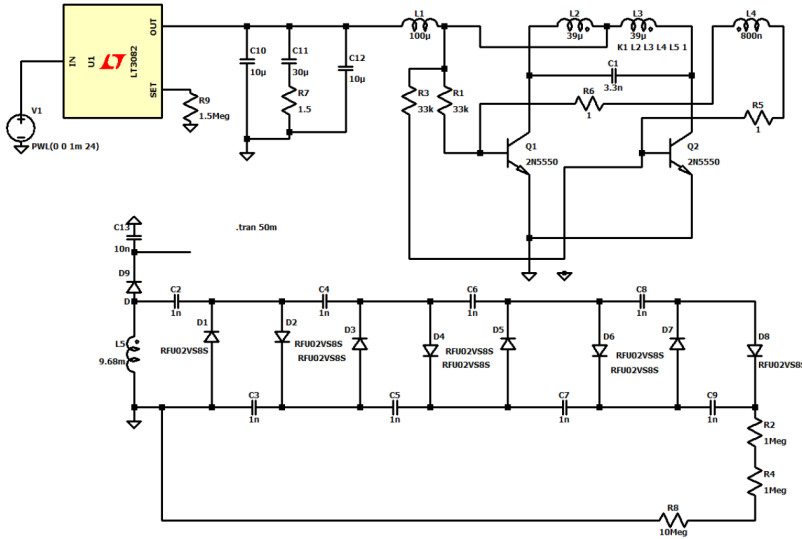
Figure 3-1 Royer based DC/DC converter convert 24V to 2.5 kV

This design utilizes a Resonant Royer oscillator, which consists of two transistors with their collectors connected to a center-tapped transformer. The circuit is self-oscillating, generating a sinusoidal voltage in the transformer's secondary winding. A significant advantage of Royer oscillators is their ability to produce low-noise voltage with minimal harmonic content. Figure 3-2 illustrates a specific variant of this Royer oscillator [23].

Figure 3-2 Royer oscillator

The operational principle of this circuit can be comprehended as follows: When transistors Q1 and Q2 conduct, inductors L2 and L3 generate a magnetic field in the transformer. This magnetic field induces a voltage of opposite polarity in L4, thereby reducing the base voltage of Q1 and Q2 until they switch and conduct in the opposite direction. Adjusting the value of C1 allows for control over the oscillation frequency. It is important to note that the transistors always conduct in a unidirectional manner.
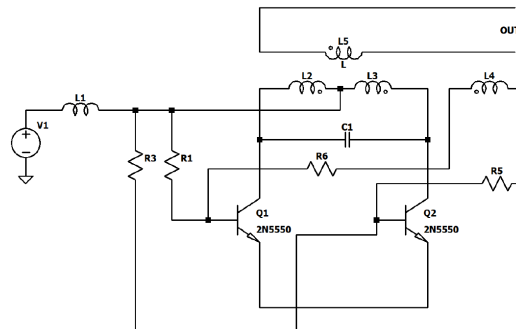
However, the circuit lacks a feedback loop, which results in output variations due to the temperature dependence of the transistors. Moreover, the circuit's sensitivity to input voltage fluctuations necessitates the use of a costly linear voltage regulator for stable operation. These challenges highlight areas for potential improvement in the design.

3.3 High-frequency Royer-based converter

The converter design presented in figure 3-3 use of a planar air-core transformer instead of a conventional transformer. Planar transformers, which consist of coils with all turns in the same plane, are employed to form the primary and secondary sides of planar transformers. For instance, these inductors can be integrated into a printed circuit board (PCB) by tracing two coils in separate layers stacked on top of each other. Planar transformers offer several advantages over conventional transformers, the primary being their simplicity, affordability, and ease of mass production. Additionally, the thin and wide copper traces in PCBs result in reduced losses due to the skin effect compared to traditional copper wires.

This design allows planar transformers to operate effectively at very high frequencies even without an iron core. The inductances and coupling factor of the transformer are influenced by its

geometry and the permeability of the core. The relationship between mutual inductance (M), coupling factor (k), and self-inductances (Li) is given by $M = k \sqrt{(L1L2)}$.

The transformer's design was dictated by size requirements detailed in previous Chapter, with the secondary side's outer diameter capped at a maximum of 3 cm. The PCB substrate was extended beyond the transformer's edge to prevent arcing. Key considerations in the design included resistive losses and the transformer's coupling factor. The resistance of the transformer windings was calculated based on the width, length, and depth of the copper traces on the PCB. To reduce winding resistance while maintaining the number of turns, the secondary coil was divided into two equal parts and placed in adjacent PCB layers. Consequently, the transformer's layer configuration was secondary winding first half (top), secondary winding second half (middle), and primary winding (bottom).
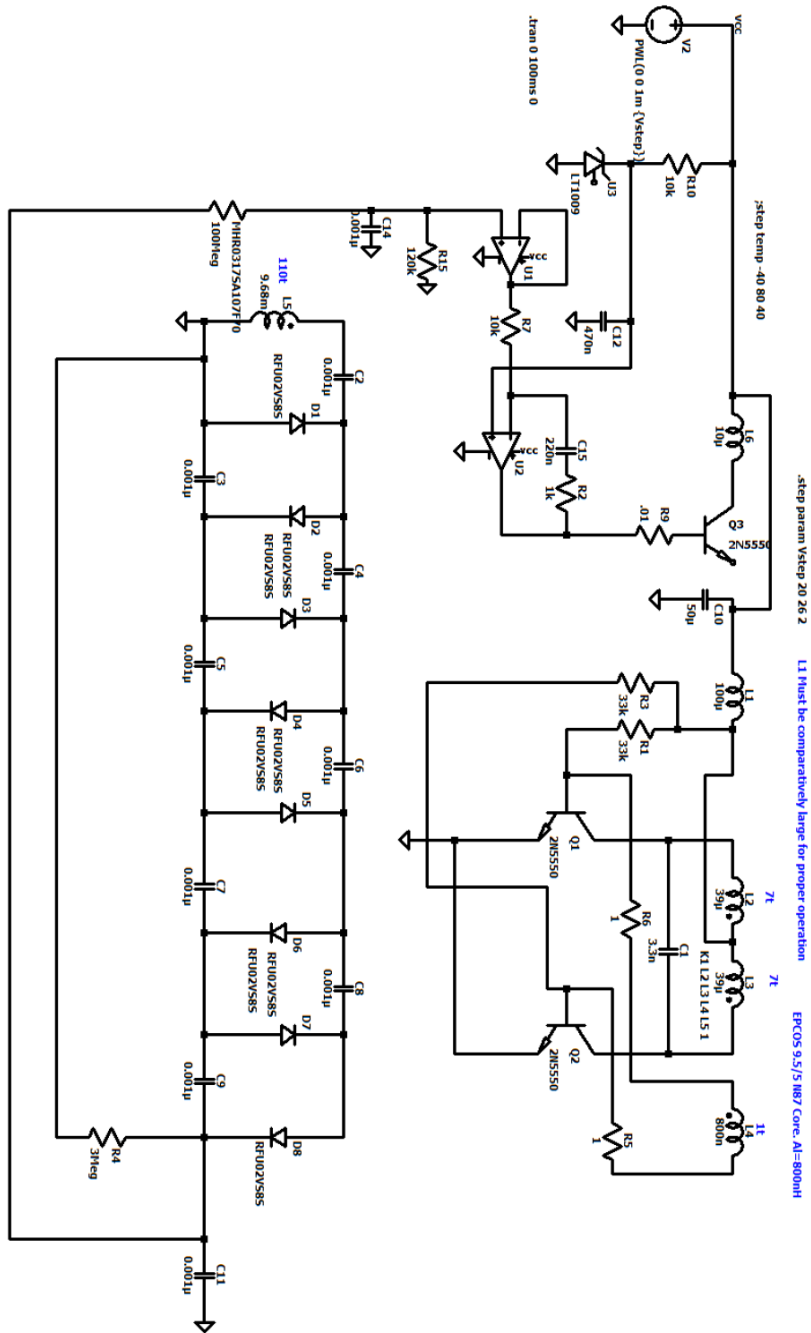
Figure 3-3 Conventional Royer-based converter LT-spice schematic

The theoretical coupling factor, self-inductances (L1 and L2), and mutual inductance (M) of the transformer were calculated using equation 7 and the method described in Chapter 2.6, yielding L1 = 570 nH, L2 = 42 µH, M = 3.9 µH, and k = 0.80. The accuracy was set to 0.1% (ND = 10) based on the method's creators. Dimensions and calculated quantities are summarized in Table 3-1.

	Primary coil	Secondary coil
Number of turns	5	26
Outer radius [mm]	15	15
Inner radius [mm]	6	6
Copper thickness [µm]	70	35
Substrate thickness [mm]	1.6	1.6
Self-inductance [µH]	0.57	42

Table 3-1 Planar PCB transformer parameters and calculated self-inductances. The mutual inductance and the coupling factor were calculated to 3.9 µH and 0.80, respectively.
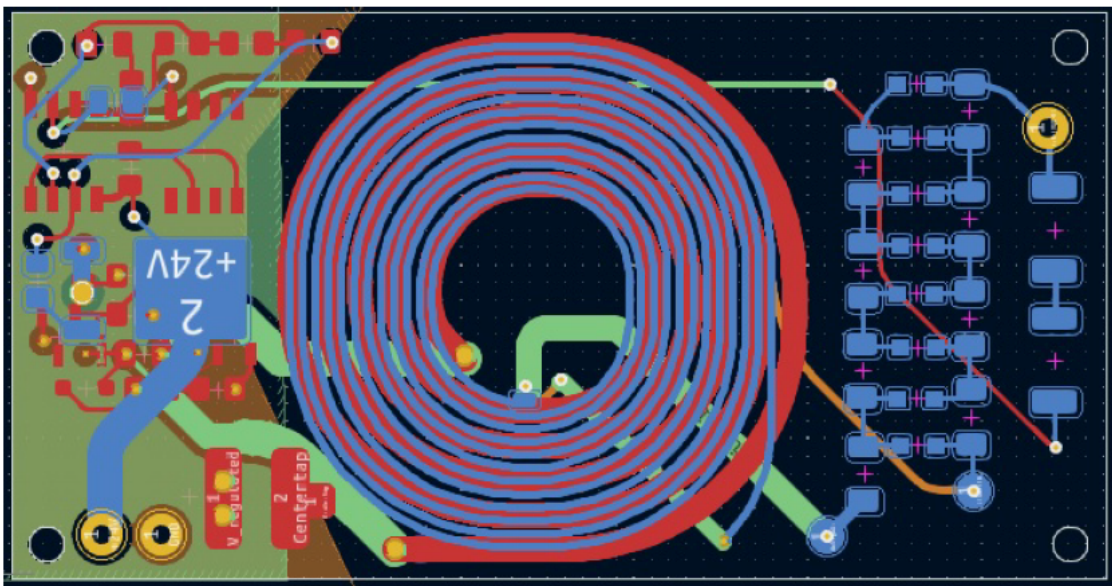
Figure 3-4: The PCB layout of the high-frequency Royer converter features circular traces forming the planar transformer.

In the PCB layout, the red trace represents the primary winding located on the front of the PCB, while the blue trace represents half of the secondary winding on the back of the PCB. The other half of the secondary winding is placed directly under the blue trace on an inner layer of the PCB. The PCB dimensions are 6.3 x 3.3 cm.

3.4 High-frequency Royer-based converter

In this topology, the DC input voltage is first increased using a boost converter, then inverted. The AC output from the inverter is connected to a capacitor-diode voltage multiplier, which further increases and rectifies the voltage. The primary advantage of this design is the elimination of a transformer for the initial voltage increase, reducing the converter's weight and size.
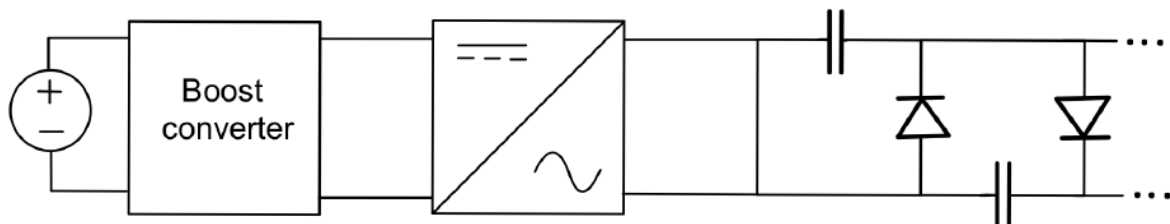

Figure 3-5 Converter topology consisting of a boost converter followed by an inverter followed by a voltage multiplier bridge.

The boost converter was set to operate at its maximum frequency of 500 kHz. To meet the safety standard specified in section 6, "Protection against electric shock", the capacitors in the

Cockcroft-Walton bridge were chosen with the largest possible capacitance, ensuring the total charge did not exceed 45 μC. The total charge was calculated as follows:

$$Q = \hat{U}_{in} \cdot C \cdot N_C \cdot 1.1$$

where U^in is the peak pulsating voltage entering the voltage multiplier, C is the capacitance for each capacitor, NC is the total number of capacitors in the bridge, and 1.1 accounts for a 10% tolerance in the capacitors.

A target output voltage of 112V from the LT8331 was chosen to provide a 20% safety margin below the maximum output voltage of 140V. According to the calculation, 18 stages were initially required to achieve an output voltage of 2 kV. However, simulation results indicated that 22 stages were needed when considering the maximum allowed charge in the voltage multiplier. The input voltage to the bridge, or the output from the LT8331, was determined to be 111V.

$$C = \frac{Q}{\hat{U}_{in} \cdot N_C \cdot 1.1} \approx 8.6\,\text{nF}$$

The E12 standard value of 8.2 nF was selected, resulting in a total charge of approximately 42.7 μC. The final circuit configuration is shown in Figure 3-6. Comparison with equation 3, which accounts for voltage drop, confirmed that 22 stages were necessary to reach 2 kV. For the Series positive-negative voltage multiplier, the stages are halved, considering one of the parallel voltage multipliers, and the output voltage is then doubled for accuracy.
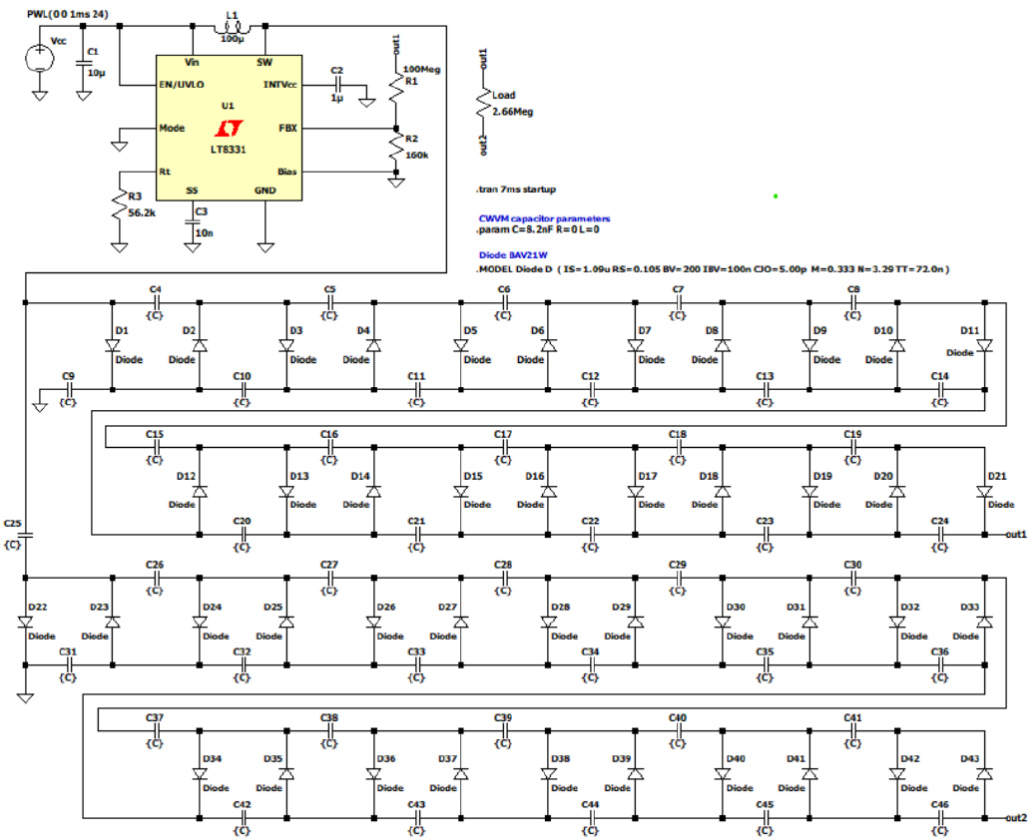
Figure 3-6 Boost Converter Combined with a 22-Stage Voltage Multiplier
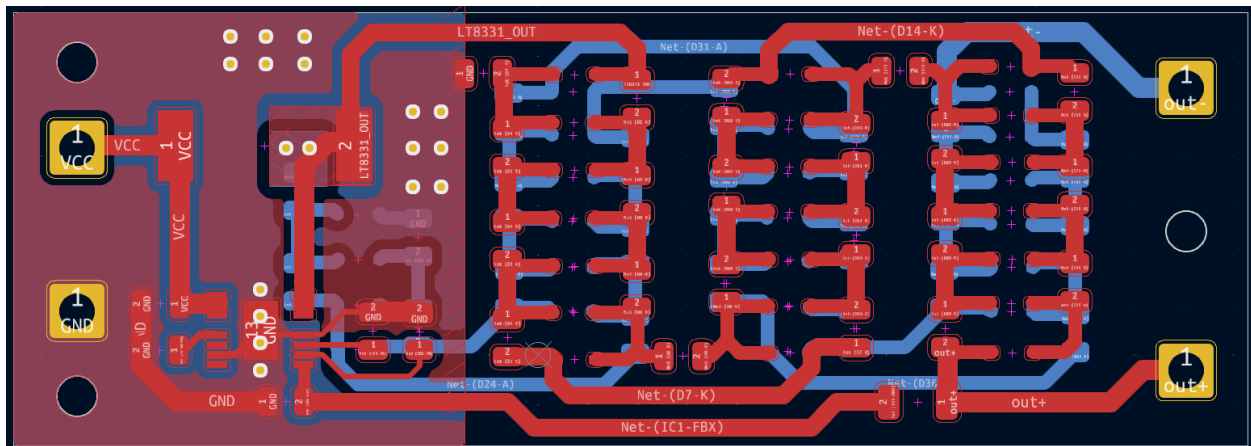

Figure 3-7 PCB layout of the transformerless DC-DC converter.

18

The PCB for this transformer less converter was designed for the circuit with capacitors of equal

capacitance and the dimensions are 6.21 cm * 2.21 cm. Its layout is shown in figure 3-7.
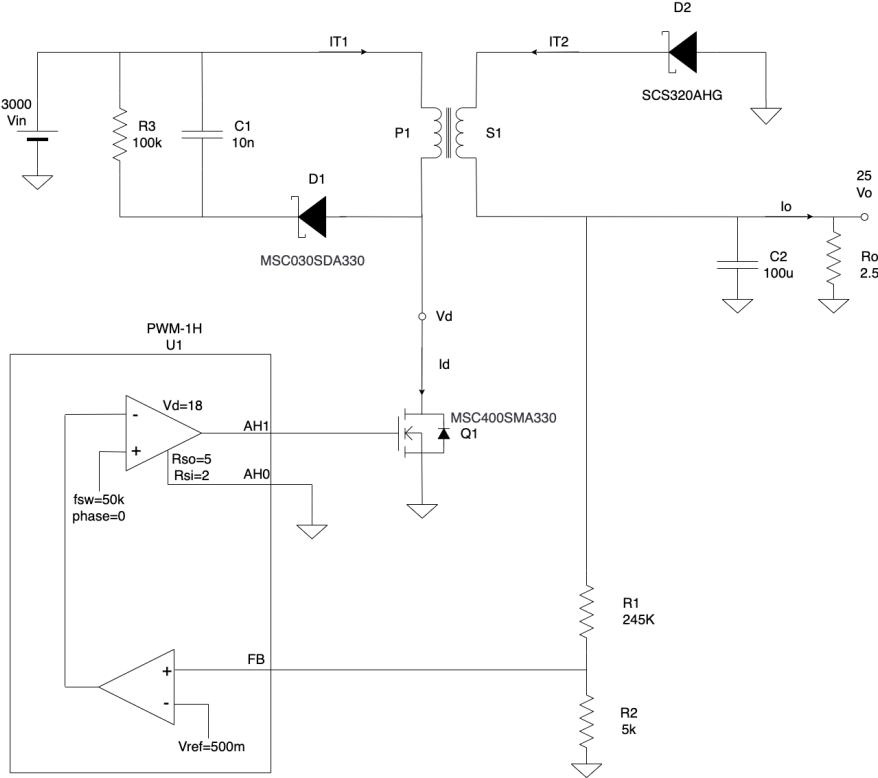
Figure 3-8 Flyback DC-DC converter from 3kV-24V.

CHAPTER 4: ANALYSIS

4.1 High-frequency Royer converter utilizing a planar transformer with an air core

The circuit operated at a switching frequency of approximately 2.8 MHz across all test cases. After 5 ms of simulation under standard conditions detailed in previous chapter. the circuit's output voltage stabilized around 2 kV in each scenario. The circuit's efficiency showed minimal sensitivity to temperature variations. Refer to figure 4-1 for a visual representation of these findings.

Figure 4-1Output voltage for −40 ◦C, 0 ◦C, 40 ◦C and 80 ◦C from the high frequency Royer-based converter. The efficiency was almost unaffected by temperature.

The circuit was tested in simulation with input voltages of 16V, 18V, 20V, 22V, 24V, and 26V, all conducted at the standard LTspice temperature of 27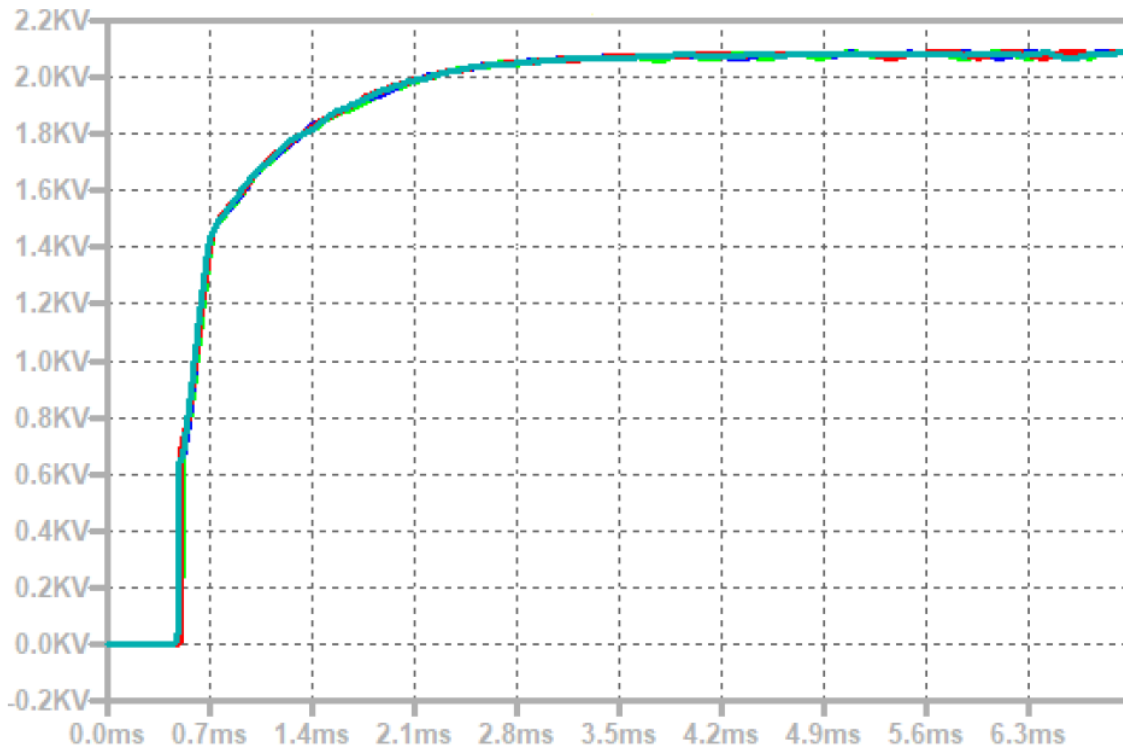°C. Approximately 5 ms after initiation, each input voltage achieved an output voltage of around 2 kV. The circuit demonstrated efficiency ranging from 40% to 75%. The power delivered to the load measured 1.45W for input voltages of 18V, 20V, 22V, 24V, and 26V, while for 16V input voltage, it was 1.24W. Refer to Table 3 and Figure 4-2 for a detailed presentation of these outcomes.

Input voltage [V]	16	18	20	22	24	26
Steady state V_{out} [V]	2002	2082	2084	2086	2086	2088
Efficiency [%]	68	60	56	48	45	41
P_{out} [W]	1.24	1.45	1.45	1.45	1.45	1.45

Table 4-1 Characteristics of the Royer air core converter for six input voltages, at 27 ∘C.

21
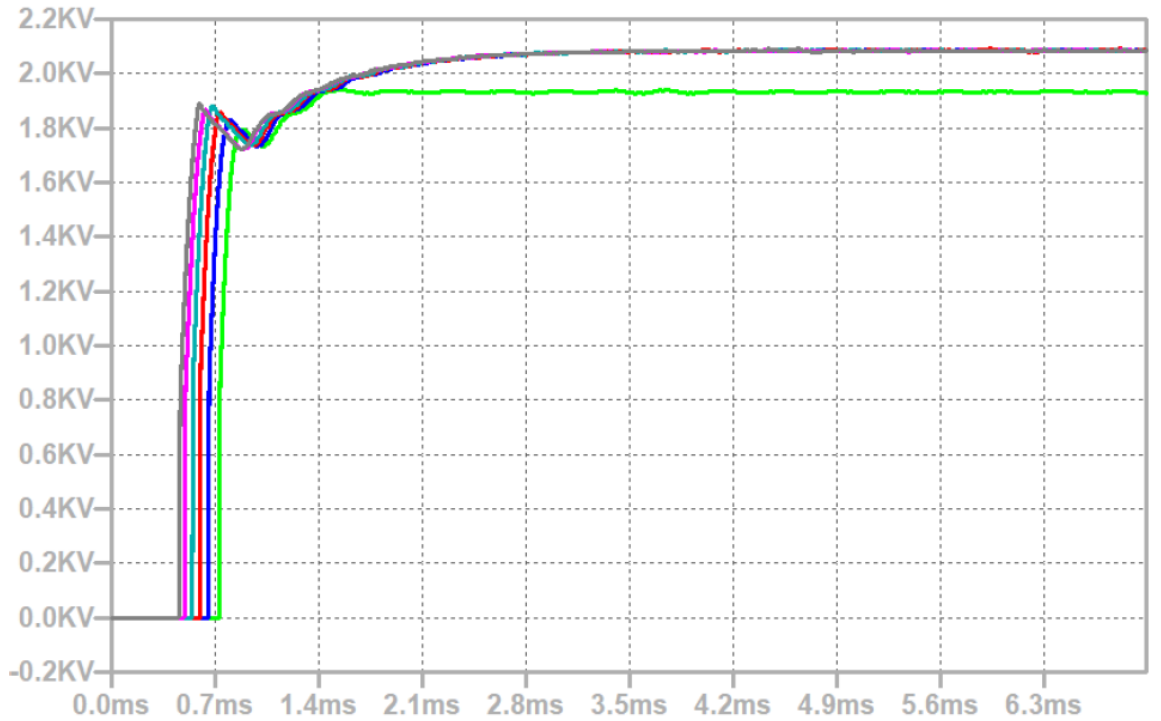
Figure 4-2 Output voltage for input voltages 16V, 18V, 20V, 22V, 24V and 26V from the high-frequency Royer converter in figure

4.2 Transformerless converter

The switching frequency remained around 500 kHz for all test cases and both circuit variants. Figure 4-3 illustrates a comparison of the output voltage and rise time across temperatures ranging from -40°C to 80°C. The rise time measured approximately 2.8 ms across all temperatures, with testing conducted using a 24V input voltage. Additionally, the circuit exhibited minimal sensitivity to temperature variations in terms of efficiency.
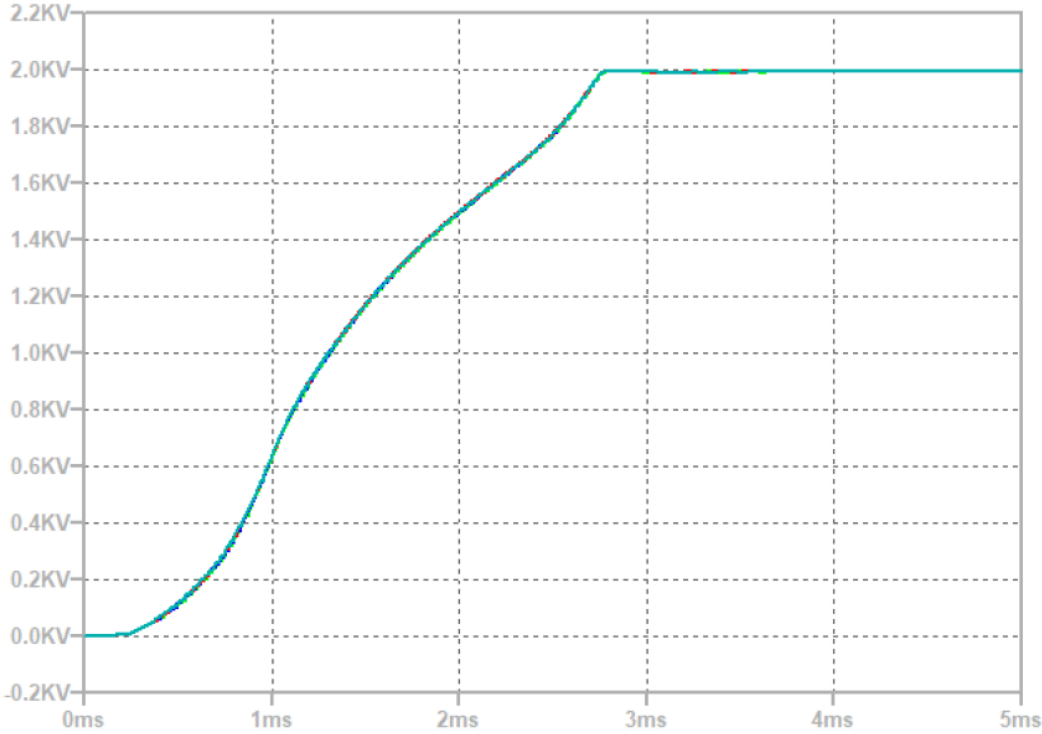
Figure 4-3 Output voltage for temperatures −40 ∘C (pink), 0 ∘C (turquoise), 40 ∘C (red) and 80 ∘C (blue) from the DC-DC converter. The input voltage was 24V for every temperature text

Both variants of the circuit were simulated using input voltages of 12V, 24V, 36V, and 48V at the standard LTspice temperature of 27°C. After 4 ms of simulation time, both circuits achieved a stable output voltage of approximately 2 kV.

The efficiency ranged from 55.79% to 91.59% with the optimized bridge configuration. For detailed results of the converter with equal capacitances, refer to Figure 4-4 and Table 4-2.
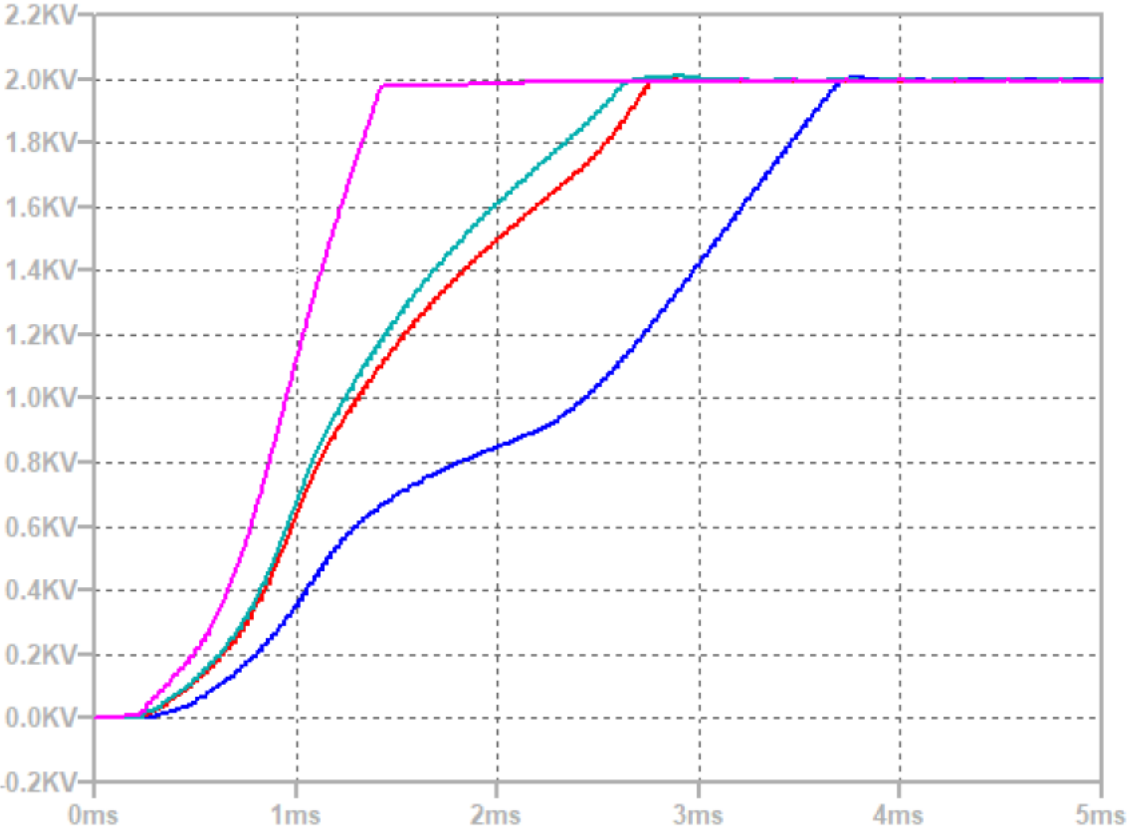
Figure 4-4 Output voltage for input voltages 48V (pink), 36V (turquoise), 24V (red) and 12V (blue) from the DC-DC converter

Input voltage [V]	12	24	36	48
Steady state V_{out} [V]	1979	1976	1978	1975
Efficiency [%]	55.79	91.59	90.09	82.04
P_{out} [W]	1.472	1.469	1.471	1.467
Output ripple. [V]	2.799	1.976	1.977	1.836

Table 4-2 Characteristics of the LT8331 DC-DC converter circuit during four different input voltages. For every case, the switching frequency was 500 kHz. The standard temperature in LTspice of 27 ∘C was used for every case.

4.3 Step down Converter
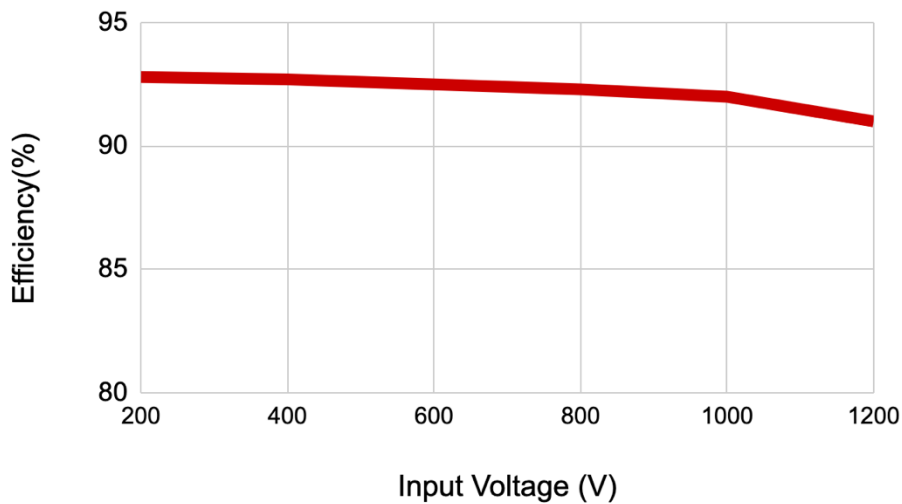
Figure 4-5 Step Down Converter Output voltage for input voltages.

The input voltage for this stage is set at 3000 volts DC, with a full load current of 50 milliamperes. The output voltage is maintained at 25 volts, while the output current is 0.6 amperes. To ensure safety, all test experiments were conducted within an isolation box. The

results indicate that as the input voltage is increased, the efficiency of the converter decreases.

Nevertheless, the average efficiency remains at approximately 92% as shown in figure 4-5.
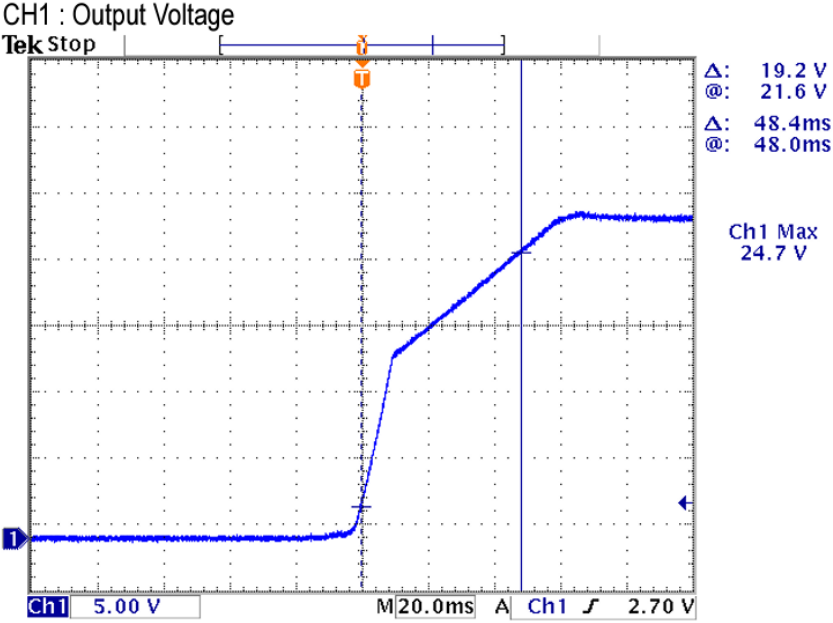
Figure 4-6 Output Voltage at Full Load

As shown in figure 4-6, under full load conditions, the rising time of the output voltage is within

50 milliseconds, and the ripple, measured at 20 millivolts, is negligible.

4.4 Prototype Set Up
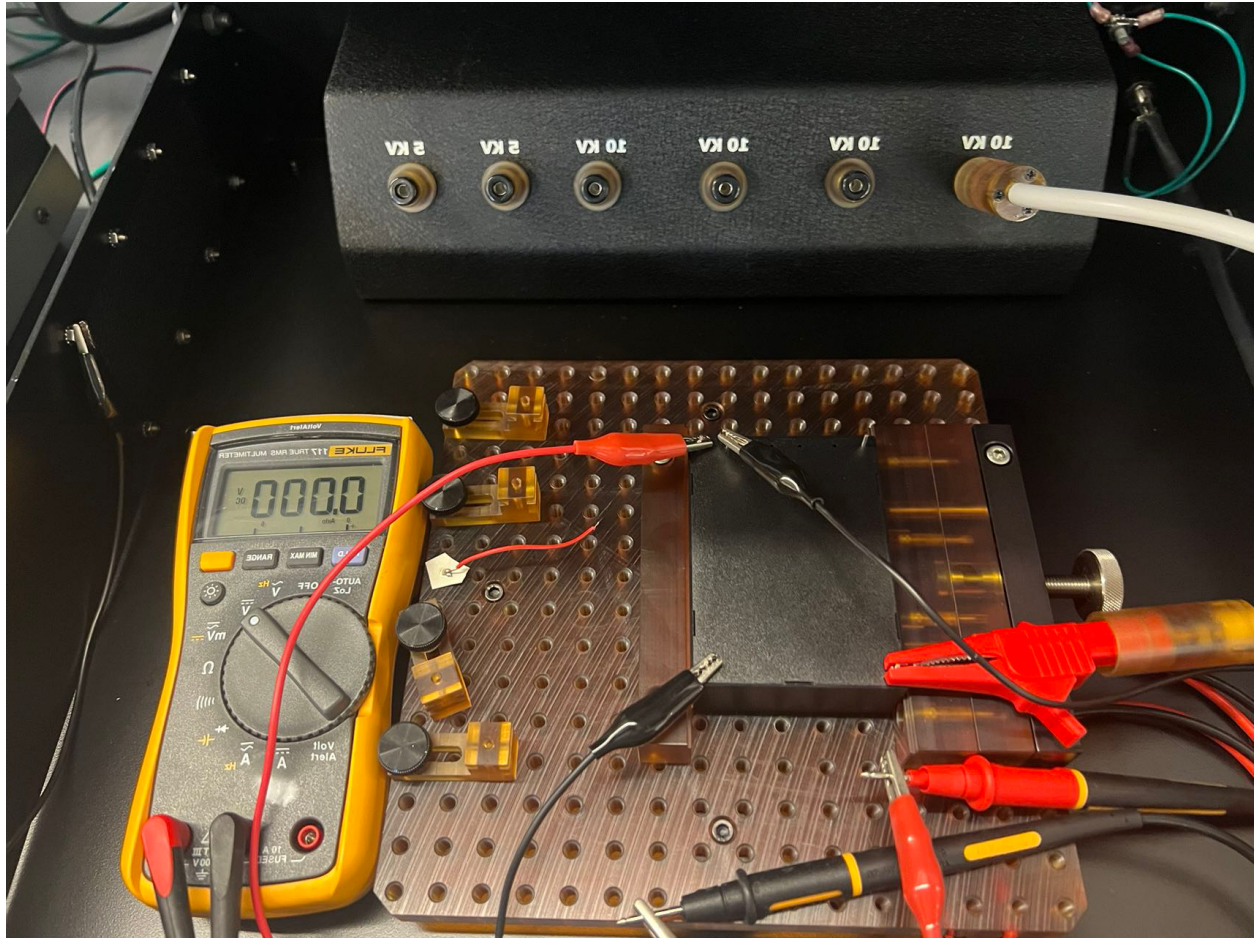
Figure 4-7 Experimental Lab Setup

1. Keithley 2290-10 High Voltage Power Supply

2. 10kV SHV male connection to 10kV banana 1.5-meter cable

3. interlock cables

4. 10 kV high voltage test fixture box (PPD3 -10kV)

This is the prototype setup of the whole project with the converters and PVDF sample capacitors.

CHAPTER 5: CONCLUSION

The high-frequency Royer-based converter met most requirements, except for efficiency and size It exceeded the size requirement due to the transformer's diameter matching the PCB's width requirement, along with the additional substrate around its edge. To fit within size limits, an oval transformer could be considered, albeit at the expense of increased complexity in calculations. Alternatively, reducing the transformer size could meet size requirements, albeit with potential performance trade-offs.

Similar to the conventional Royer-based converter, feedback stabilized the output voltage but compromised efficiency. This converter exhibited slightly lower efficiency compared to the conventional version, largely due to the use of more expensive transistors required for higher frequencies. Consequently, despite the cost benefits of the planar transformer, the overall cost of this converter was comparable to that of the conventional Royer-based design.
The transformerless converter met all requirements except for cost at input voltages of 24V, 36V, and 48V. Like the other converters discussed, the LT8331 switched boost converter used feedback to maintain a stable output voltage across various conditions.

It excelled in efficiency and accepted a wider range of input voltages compared to other converters in this study. This superior performance can be attributed to the LT8331's ability to regulate voltage through switching rather than dissipating excess energy in a feedback loop.

However, its higher cost was a significant drawback. This was primarily due to the use of the LT8331 boost converter and the large voltage multiplier, which required numerous specialized components, driving up costs beyond initial estimates. As a result, despite being transformerless, this converter did not necessarily offer a more economical solution compared to circuits incorporating transformers.

Replacing the LT8331 could potentially reduce costs and mitigate production uncertainties, although this would present technical challenges.

Considering the overcurrent protection, achieving the desired limit of 2mA peak output current was only possible with the 1MΩ series resistance in combination with the 1H series inductance, specifically in the Royer-based converter. However, using an inductor with such a large inductance would substantially increase both the cost and size of each converter discussed in this paper.

All step-up and step-down DC/DC Converters meet the perspectives. However, to achieve higher energy storage, it is necessary to make the maximum voltage which converter can achieve higher since the energy proportional to the square of voltage.

REFERENCES

[1]   Mikael Antelius et al. 'Miniature Pumped Fluid Loop Regulating Payload under Simulated Earth Albedo Heat Load on Radiator'. In: *47th International Conference on Environmental Systems*. Charleston, SC, USA, July 2017. url: http://hdl.handle.net/2346/72917.

[2]   Alex Lidow et al. '1.2 The Gallium Nitride Journey Begins'. In: *GaN Transistors for Efficient Power Conversion (3rd Edition)*. John Wiley & Sons, 2020. isbn: 978-1-11959-4-147. url: https://app.knovel.com/hotlink/khtml/id:kt0125DYR8/gan-transistors-efficient/gan-sic-comparedwith.

[3]   Alex Lidow et al. '17. Replacing Silicon Power MOSFETs'. In: *GaN Transistors for Efficient Power Conversion (3rd Edition)*. John Wiley & Sons, 2020. isbn: 978-1-11959-4-147. url: https://app.knovel.com/hotlink/khtml/id:kt0125E6C1/gan-transistors-efficient/new-capabilitiesenabled.

[4]   Alex Lidow et al. '3. Driving GaN Transistors'. *In: GaN Transistors for Efficient Power Conversion (3rd Edition)*. John Wiley & Sons, 2020. isbn: 978-1-11959-4-147. url: https://app.knovel.com/hotlink/khtml/id: kt0125DZL1/gan-transistors-efficient/driving-ga-introduction.

[5]   Jim Williams. *High Voltage, Low Noise, DC/DC Converters*. Application note. Analog Devices, Mar. 2008. url: https://www.analog.com/media/en/technical-documentation/application-notes/an118fb.pdf.

[6]   Mojtaba Forouzesh et al. 'Step-Up DC–DC Converters: A Comprehensive Review of Voltage-Boosting Techniques, Topologies, and Applications'. In: *IEEE Transactions on Power Electronics* 32.12 (2017), pp. 9143–9178. doi:10.1109/TPEL.2017.2652318.

[7]   Boris Axelrod, Yefim Berkovich and Adrian Ioinovici. 'Switched-Capacitor/Switched-Inductor Structures for Getting Transformerless Hybrid DC–DC PWM Converters'. In: *IEEE Transactions on Circuits and Systems I: Regular Papers* 55.2 (2008), pp. 687–696. doi: 10.1109/TCSI.2008.916403.

[8]   Sanghyeon Park, Jun Yang and Juan Rivas-Davila. 'A Hybrid Cockcroft–Walton/Dickson Multiplier for High Voltage Generation'. In: *IEEE Transactions on Power Electronics* 35.3 (2020), pp. 2714–2723. doi: 10.1109/TPEL.2019.2929167.

[9]   Gaetano Palumbo and Domenico Pappalardo. 'Charge Pump Circuits: An Overview on Design Strategies and Topologies'. In: IEEE *Circuits and Systems Magazine* 10.1 (2010), pp. 31–45. doi: 10.1109/MCAS.2009.935695

[10]   I.C. Kobougias and E.C. Tatakis. 'Optimal design of a Half-Wave Cockroft-Walton Voltage Multiplier with minimum total capacitance'. In: *2008 IEEE Power Electronics Specialists Conference*. 2008, pp. 1104–1109. doi: 10.1109/PESC.2008.4592077.

[11]   J.S. Brugler. 'Theoretical performance of voltage multiplier circuits'. In: *IEEE Journal of Solid-State Circuits* 6.3 (1971), pp. 132–135. doi: 10.1109/JSSC.1971.1049670.

[12]   Naseer Ahmed, Noman Khan and Tanveer Abbas. 'An Inverter-Fed Cockcroft-Walton Multiplier Based High Voltage DC Source for Tokamak'. In: *2022 International Conference on Emerging Trends in Electrical, Control, and Telecommunication Engineering (ETECTE)*. 2022, pp. 1–6. doi: 10.1109/ETECTE55893.2022.10007169.

[13]   Christian Maennel. 'Improvement in the modelling of a half-wave Cockroft-Walton voltage multiplier'. In: *The Review of scientific instruments 84* (June 2013), p. 064701. doi:10.1063/1.4807703.

[14]   Mohsen Ruzbehani. 'A Comparative Study of Symmetrical Cockcroft-Walton Voltage Multipliers'. In: *Journal of Electrical and Computer Engineering 2017* (Jan. 2017), pp. 1–10. doi: 10.1155/2017/4805268.

[15]   *Low IQ boost/SEPIC/Flyback/Inverting Converter with 0.5A, 140V Switch.* LT8331. Rev. C. Linear Technology. 2015. url: https://www.analog.com/media/en/technical-documentation/data-sheets/LT8331.pdf.

[16]   Lew Andrew R. Tria, Daming Zhang and John E. Fletcher. '*Planar PCB Transformer Model for Circuit Simulation*'. In: IEEE Transactions on Magnetics 52.7 (2016), pp. 1–4. doi:10.1109/TMAG.2016.2516995.

[17]   Sanghyeon Park, Lei Gu and Juan Rivas-Davila. 'A Compact 45 V-to-54kV Modular DC-DC Converter'. In: *2019 20th Workshop on Control and Modeling for Power Electronics (COMPEL)*. 2019, pp. 1–7. doi: 10.1109/COMPEL.2019.8769612.

[18]   William Gerard Hurley et al. 'A Unified Approach to the Calculation of Selfand Mutual-Inductance for Coaxial Coils in Air'. In: *IEEE Transactions on Power Electronics* 30.11 (2015), pp. 6155–6162. doi: 10.1109/TPEL.2015.2413493.

[19]   M.M GÅLongora-Nieto et al. 'Impact of air bubbles in a dielectric liquid when subjected to high field strengths'. In: *Innovative Food Science & Emergin Technologies* 4.1 (2003), pp. 57–67. issn: 1466-8564. doi: https://doi.org/10.1016/S1466-8564(02)00067-X. url: https://www.sciencedirect.com/science/article/pii/S146685640200067X.

[20]   'IEEE Guide for Reliability-Based Placement of Overhead and Underground Switching and Overcurrent Protection Equipment up to and Including 38 kV'. In: *IEEE Std 1806-2021* (2021), pp. 1–52. doi: 10.1109 / IEEESTD .2021.9508912.

[21]   Younsi Abdelkrim et al. 'Electrostatic Precipitator Having a Spark Current Limiting Resistors and Method for Limiting Sparking'. US 2011/0005388 A1. 13th Jan. 2011.

[22]   Henry Ibekwe. 'Realization of a low-cost Op-Amp based PID Controller'. In: (June 2018). doi: 10.13140/RG.2.2.29981.00485.

[23]   TDK Electronics. 'Ferrites and accessories ER 9.5/5'. In: (2022). url: https://www.sciencedirect.com/science/article/pii/S146685640200067X.

[24]   Nor Azmi et al. '5 V to 6 kV DC-DC Converter Using Switching Regulator with Cockcroft-Walton Voltage Multiplier for High Voltage Power Supply Module'. In: *Recent Advances in Electrical & Electronic Engineering (Formerly Recent Patents on Electrical & Electronic Engineering)* 11 (June 2018). doi: 10.2174/2352096511666180605094827.

[25]   Sohiful Anuar Zainol Murad et al. 'A Novel 1.6 kV High Voltage Low Current Step-Up DC-DC Converter with Cockroft-Walton Voltage Multiplier for Power Supply Modules'. In: Jurnal Teknologi 81 (Aug. 2019). doi: 10.11113/jt.v81.13411.

[26]   Sanghyeon Park, Lei Gu and Juan Rivas-Davila. '60 V-to-35 kV input-parallel output-series DC-DC converter using multi-level class-DE rectifiers'. In: *2018 IEEE Applied Power Electronics Conference and Exposition (APEC)*. 2018, pp. 2235–2241. doi: 10.1109/APEC.2018.8341327.

[27]   Hyukjae Kwon et al. 'Analytical Modeling and Design of 27.12 MHz Single-Switch DC–DC Converter With PCB Transformer'. In: *IEEE Access 11*(2023), pp. 12742–12754. doi:10.1109/ACCESS.2023.3242010.

[28]   N. Dai et al. 'A comparative study of high-frequency, low-profile planar transformer technologies'. In: *Proceedings of 1994 IEEE Applied Power Electronics Conference and Exposition - ASPEC'94*. 1994, 226–232 vol.1. doi:10.1109/APEC.1994.316395.

[29]   BSI Standards Publication. *Safety requirements for electrical equipment for measurement, control, and laboratory use – Part 1: General requirements*.BS EN 61010-1:2010. London, UK: BSI, 2010.